Shape of spin density wave versus temperature in AFe_2As_2 (A = Ca, Ba, Eu): A Mössbauer study

A. Błachowski,[1] K. Ruebenbauer,[1,*] J. Żukrowski,[2] K. Rogacki,[3] Z. Bukowski,[4] and J. Karpinski[4]

[1]*Mössbauer Spectroscopy Division, Institute of Physics, Pedagogical University PL-30-084 Kraków, ul. Podchorążych 2, Poland*

[2]*Solid State Physics Department, Faculty of Physics and Applied Computer Science, AGH University of Science and Technology, PL-30-059 Kraków, Al. Mickiewicza 30, Poland*

[3]*Institute of Low Temperatures and Structure Research, Polish Academy of Sciences, PL-50-422 Wrocław, ul. Okólna 2, Poland*

[4]*Laboratory for Solid State Physics, ETH Zurich, CH-8093 Zurich, Switzerland*

(Received 17 January 2011; revised manuscript received 16 February 2011; published 11 April 2011)

Parent compounds AFe_2As_2 (A = Ca, Ba, Eu) of the 122 family of the iron-based superconductors have been studied by ^{57}Fe Mössbauer spectroscopy in the temperature range 4.2–∼300 K. Spin density waves (SDW) have been found with some confidence. They are either incommensurate with the lattice period or the ratio of the respective periods is far away from the ratio of small integers. SDW shape is very unconventional (i.e., differs from the sinusoidal shape). Magnetic order starts with lowered temperature as narrow sheets of the significant electron spin density separated by areas with very small spin density. Magnetic sheets are likely to be ordered in the alternate antiferromagnetic fashion as the material as a whole behaves similarly to the collinear antiferromagnet. A further lowering of temperature simply expands sheet thickness leading to the near triangular SDW. Finally, sheets fill the whole available space and the almost rectangular shape of the SDW is reached. The substantial maximum amplitude of SDW appears at the temperature just below the magnetic onset temperature, and this maximum amplitude increases slightly with lowering temperature. The square root from the mean squared hyperfine field behaves versus temperature according to the universality class (1,2) (i.e., with the electronic spin space having dimensionality equal to unity and the real space having dimensionality equal to 2). The more or less pronounced tail above transition temperature due to the development of incoherent SDW is seen.

DOI: 10.1103/PhysRevB.83.134410 PACS number(s): 74.70.Xa, 75.30.Fv, 76.80.+y

I. INTRODUCTION

Iron pnictides and chalcogenides are very interesting compounds, as by a slight variation of the atomic order and lattice parameters due to doping or applying external pressure, one can switch from antiferromagnets to the iron-based superconducting materials. The material in the metallic state can be a superconductor at low temperatures without any 3*d* magnetism[1,2] or some magnetic order develops for delocalized spins of the 3*d* electrons.[1] Iron-based pnictides AFe_2As_2 (A = Ca, Sr, Ba, Eu) are parent compounds of the 122 family of the iron-based superconductors. The parents are strongly layered intermetallic compounds developing iron-based magnetic order in contrast to the corresponding superconductors, the latter have no magnetic moment due to iron.[3] A magnetic transition is correlated with the phase transition from the high temperature tetragonal phase to the low temperature orthorhombic phase. Both transitions occur at about 170 K for A = Ca (Ref. 4), 200 K for Sr (Ref. 5), 140 K for Ba (Ref. 6), and 190 K for Eu (Ref. 5). A magnetic order in the parent compounds exhibits many unconventional features typical for the spin density wave (SDW) type of order. Other studies detected SDWs, in fact, at least for underdoped materials.[7,8] However, many studies, by methods sensitive to the local environment of the iron atom, refuted the existence of SDWs being incommensurate with the lattice period.[9,10] Bonville *et al.*[11] have found SDWs in Co-substituted (underdoped) $BaFe_2As_2$ by using Mössbauer spectroscopy. The shape of the SDW was found to be far away from the sinusoidal, in contrast to the "classical" SDW materials like chromium. Some other attempts to evaluate Mössbauer data within the framework of SDWs have been performed as well, but the assumption of the purely sinusoidal SDW shape was applied in a more or less implicit fashion.[12] Mössbauer spectra of the parent compounds of the 122 and 1111 families of iron-based superconductors in the magnetically ordered state (even close to saturation) are hard to fit by a unique set of hyperfine parameters, despite the fact that iron occupies a unique and precisely defined crystallographic position including black and white symmetry.[13–17] The black and white symmetry is due to the antiferromagnetism. Better fits are usually obtained by applying field distribution or several fields, but such a treatment has no physical background. To resolve this discrepancy we have performed studies of the AFe_2As_2 (A = Ca, Ba, Eu) compounds in the temperature range 4.2–∼300 K by using Mössbauer spectroscopy of the 14.41-keV line in ^{57}Fe. One has to note that the above compounds make the best-ordered crystals of all parents of the iron-based superconductors as their atomic composition ensures that the number of point defects is negligible.

II. EXPERIMENT

Single crystals of $CaFe_2As_2$ and $EuFe_2As_2$ were grown by the tin flux method as described in Refs. 18 and 19, respectively. The polycrystalline sample of $BaFe_2As_2$ was prepared by the solid state reaction at elevated temperature.[20] X-ray diffraction confirmed that samples are single phases of high purity.[18–20]

Mössbauer absorbers were prepared in the powder form, crushing single crystals or polycrystalline material in the mortar to micrometer-sized crystals. Powder absorbers are advantageous while seeking details of the hyperfine parameter distributions, unless perfect sufficiently thin single crystals which completely fill the absorber holder are available, as

partial orientation interferes with the hyperfine field distribution. On the other hand, hyperfine parameters (line positions) do not depend on the crystal size unless this crystal has a size that is comparable with the chemical unit cell. One cannot expect a very large coherence length of SDWs due to pinning by defects and therefore the micrometer scale of the powder grain is large compared to the average distance between defects. Powders were mixed with an ample amount of boron carbide fine powder to assure as random as possible orientation of crystallites and then lightly pressed between mylar sheets aluminized on both sides. About 55 mg of AFe_2As_2 material was used to make the absorber, which had a 16 mm diameter with a 12 mm clear bore. Absorbers were mounted on the gold-plated copper holder equipped with the thermometer and heater. A Janis Research Co. Inc. cryostat SVT-400M was used with the sample either immersed in the liquid helium under almost ambient pressure or exposed to the nitrogen vapor flow. For the latter case the heater was used to maintain the desired temperature. The long-range temperature stability and homogeneity was better than 0.01 K except for room temperature (RT) and 4.2 K, where the temperature was not stabilized. A commercial source ^{57}Co(Rh) from Ritverc G.m.b.H. was attached to the transducer and maintained at ambient temperature. Spectra were collected by means of the RENON MsAa-3 spectrometer with the velocity scale calibrated by the Michelson-Morley interferometer equipped with a metrological quality He-Ne laser. Calibration data were corrected for the beam divergence. The round-corner triangular mode of the spectrometer operation was applied. An LND Inc. Kr-filled proportional detector with an iron-free beryllium window was used to detect γ rays. All shifts of the spectra are reported here versus room temperature α-Fe. No signal from iron located in phases other than the investigated compound was found for all samples used.

III. MÖSSBAUER SPECTRA EVALUATION WITHIN SDW MODEL

The SDW represents the stationary periodic field of the electron spin density within the crystal lattice. It is assumed that the hyperfine magnetic (induction) field seen by the atomic nucleus at some (average) position **r** of the crystal lattice is proportional to the SDW amplitude at the same position (some constant angle between the SDW amplitude and hyperfine field cannot be excluded). The proportionality constant (usually) strongly depends on the kind of atom due to the atomic shell polarization. Hence, the problem can be considered as time independent. In general, one can express the amplitude of the SDW (hyperfine field **B**) by the following expression:

$$\mathbf{B}(\mathbf{r}) = \sum_{hkl=0}^{HKL} \mathbf{b}_{hkl} \cos[hq_a \mathrm{x} + kq_b \mathrm{y} + lq_c \mathrm{z} + \Phi_{hkl}] \quad \text{with} \quad \mathbf{r} = \begin{pmatrix} \mathrm{x} \\ \mathrm{y} \\ \mathrm{z} \end{pmatrix}. \tag{1}$$

Here, the indices hkl stand for the Miller indices of the crystal lattice considered, while the symbols HKL denote the maximum values of the respective Miller indices. The symbol $\mathbf{b}_{hkl}$ stands for the amplitude of the particular hyperfine field component due to the Miller indices hkl, while the symbols q_a, q_b, and q_c stand for the SDW wave-vector components along the principal crystal axes **a**, **b**, and **c**, respectively. The symbol Φ_{hkl} denotes the relative phase angle of the respective SDW component, the latter having the definite Miller indices set hkl. The coordinates xyz are defined in the principal crystal axes system **a**, **b**, and **c**, respectively. The average atomic (nuclear) positions within the crystal lattice are expressed as $(n_a + u)$a,$(n_b + v)$b, and $(n_c + w)$c along their respective crystal axes. The symbols n_a, n_b, n_c denote the relative position of the particular chemical unit cell, while the symbols u, v, w denote the fractal coordinates of the particular atom (site) within a cell. The symbols a,b,c stand for the respective lattice constants. The SDW is commensurate provided $(2\pi)^{-1} q_a$a,$(2\pi)^{-1} q_b$b and $(2\pi)^{-1} q_c$c are rational numbers. Otherwise, the SDW is incommensurate. It is hard to distinguish these two behaviors for above rational numbers being far away from the (irreducible) ratio of small nonzero integers. To get reliable results some simplifications are usually necessary. It has been assumed that a resonant atom occupies a unique position within the chemical unit cell. Furthermore, it has been assumed that the SDW is collinear and of the (normal) antiferromagnetic character. The last assumption allows for the replacement of the axial vector **B** by corresponding pseudoscalar B remembering that the sign of the hyperfine field is inaccessible in the experimental arrangement used. The assumption about collinear antiferromagnetic behavior leads to another simplification allowing for the replacement of three Miller indices by a single index n and leading to the replacement of vectors $\mathbf{b}_{hkl}$ by pseudoscalars. Finally, it has been assumed that the SDW has a similar symmetry as the previously observed SDW in chromium. The latter SDW could be expanded in the sine functions (SDW has definite parity) with odd components solely. The first condition is satisfied for any collinear antiferromagnetic SDW, while the second condition means that each half-period (without global phase shift) has midpoint mirror symmetry. Hence, the following expression has been finally adopted:[11,21]

$$B(qx) = \sum_{n=1}^{N} h_{2n-1} \sin[(2n-1)qx]. \tag{2}$$

The symbols h_{2n-1} denote amplitudes of subsequent harmonics. The symbol q stands for the wave number of SDW, while the symbol x denotes the relative position of the resonant nucleus along the propagation direction of the stationary SDW. The index N enumerates the maximum relevant harmonic. The argument qx satisfies the following condition $0 \leqslant qx \leqslant 2\pi$ due to the periodicity of the SDW. In fact, complete information is obtained having calculated expression (2) within the range $0 \leqslant qx \leqslant \pi/2$. The above range strictly applies to incommensurate conditions, but it could be used to commensurate SDW with $(2\pi)^{-1} qd$ being far away from the ratio of small nonzero integers, where the symbol d denotes the smallest distance between the various (all equivalent) resonant atoms (sites) in the direction of the propagation of SDW. The amplitude of the first harmonic h_1 is, by definition, positive, as the absolute phase shift between the SDW and the crystal lattice is generally unobservable by the method used. The average amplitude $\langle B \rangle$ of SDW

described by expression (2) equals zero, of course, while the mean squared amplitude of the above SDW is expressed as $\langle B^2\rangle = \frac{1}{2}\sum_{n=1}^{N} h_{2n-1}^2$ (Ref. 11). The last parameter is finite for any physical shape of SDW even for the infinite number of harmonics involved. One has to remember that the spectrum is sensitive to $|B(qx)|$. Equation (2) applies to the SDW of reduced dimensionality as well, provided some local method of observation is used. Amplitudes of subsequent harmonics have been fitted to the spectral shape. The remaining hyperfine parameters were used as common for all resonant sites. The electric quadrupole interaction was treated in the first order approximation, as it is small compared to the magnetic interaction for all relevant cases. It was assumed that samples have neither magnetic nor crystallographic order on the macroscopic scale. Spectra were processed by means of the GMFPHARM program in the standard transmission integral approximation. This program belongs to the MOSGRAF-2009 suite.[22] The field distribution as seen by resonant atoms can be calculated provided all relevant amplitudes of expression (2) have been determined. The distribution [i.e., probability density function $\rho(B) \geqslant 0$] takes on the form[21]

$$\rho(B) = N_0^{-1}\sum_{L(B)}\frac{\partial}{\partial B}\{\hat{B}^{-1}[|B(qx)|]\} \quad \text{with}$$

$$N_0 = \int_0^{B_{\max}} dB \sum_{L(B)}\frac{\partial}{\partial B}\{\hat{B}^{-1}[|B(qx)|]\}. \tag{3}$$

The symbol $B_{\max}$ stands for the maximum hyperfine field due to SDW. It has to be noted that operator $\hat{B}^{-1}$ is generally nonunique except within the limited ranges of the primary argument qx. Hence, the summation goes over all ranges of B with the summation index $L(B)$ being dependent on the actual value of B. The number of ranges is always finite and accountable. It is sufficient to consider the primary argument qx from the range $0 \leqslant qx \leqslant \pi/2$. The secondary argument B is nonnegative and upper bound. A distribution described by Eq. (3) has singularities (singular maxima) at the smooth extrema of the function described by expression (2). The singularity at the maximum of function (2) has a sharp edge above singularity, while the singularity at the minimum of function (2) has a sharp edge below singularity. The maxima of the distribution occur also at the smooth inflection points of function (2). They are singular provided $\partial B/\partial(qx) = 0$ at this point. All the above singularities are integrable (distribution is integrable and hence it is normalized), they are separated one from another, and one has a finite number of such singularities. Singularities (maxima) might overlap for some SDW shapes. Therefore it is practical to approximate the "exact" distribution given by Eq. (3) by the following expression removing singularities:

$$\rho_A(B) = \alpha^{-1}\left(\frac{1}{\Delta B}\right)\int_{B-\frac{1}{2}\Delta B}^{B+\frac{1}{2}\Delta B} dB'\rho(B') \quad \text{with}$$

$$\alpha = \int_{\frac{1}{2}\Delta B}^{B_{\max}-\frac{1}{2}\Delta B} dB\left\{\left(\frac{1}{\Delta B}\right)\int_{B-\frac{1}{2}\Delta B}^{B+\frac{1}{2}\Delta B} dB'\rho(B')\right\} \quad \text{and}$$

$$\frac{1}{2}\Delta B \leqslant B \leqslant B_{\max} - \frac{1}{2}\Delta B. \tag{4}$$

The last expression converges to Eq. (3) provided $\Delta B \to 0$. In fact, expression (4) generates a histogram (with equal steps), the latter approximating distribution described by Eq. (3). Such a histogram is adequate due to the limited resolution of the spectrum (experimental data) provided it is sufficiently dense. A distribution (probability density function) equals null for fields higher than $B_{\max}$, of course. It is interesting to note that the rectangular SDW leads to the distribution having the character of the Dirac delta function, while the triangular SDW leads to the distribution being completely flat. For purely sinusoidal SDW (all amplitudes equal zero except h_1) one gets $\rho(B) = [2/(\pi B_{\max})][1-(B/B_{\max})^2]^{-1/2}$ with $B_{\max} = h_1$. An integrable singularity appears for $B = B_{\max}$. This singularity has a sharp edge for fields above $B_{\max}$. It has to be mentioned that the wave number of SDW is inaccessible experimentally to local methods like the Mössbauer spectroscopy. Expression (2) can be applied regardless of the angle between the hyperfine field and the propagation direction of the SDW provided the above angle remains constant. In general distributions described by Eq. (3), and subsequently by expression (4), are experimentally defined for the correlation between the SDW and the crystal lattice being random. In such a case expression (2) is exact as well. The above random correlation conditions are satisfied for most cases with the SDW being incommensurate. Finally, one has to observe that Mössbauer spectroscopy is one of the best methods to look upon details of the shape of SDW provided hyperfine fields are sufficiently large. Histograms generated by Eq. (4) are presented here in the form $W(B) \sim \rho_A(B)\Delta B$ (with constant and positive ΔB) to conform to the standard presentation of the field distribution by Mössbauer spectroscopists. Each histogram $W(B)$ is normalized to unity. It has to be mentioned that a spectrum due to the single field (or several precisely defined fields) cannot be fitted within the above model. The reason for this is as follows: such a spectrum corresponds to the ideal rectangular SDW, where one has a logarithmically divergent sum of amplitudes.

IV. RESULTS AND DISCUSSION

Figure 1 shows spectra obtained in the nonmagnetic region and slightly above the magnetic ordering temperature. Some onset of the magnetic order could be detected in the lowest temperature spectra of this region, as fits without a hyperfine magnetic field are definitely of poorer quality. On the other hand, the field is too small to be reliably included in the data processing. Spectra were fitted with either a symmetric doublet or singlet. The singlet was used for a $BaFe_2As_2$ compound, as no discernible splitting exists above the magnetic ordering temperature for this compound. Some slight preferential orientation can be seen in the case of doublets—particularly for the $CaFe_2As_2$ compound with the largest quadrupole splitting. This orientation is too weak to have a significant effect in the magnetically ordered region. All relevant parameters extracted from the data obtained in the nonmagnetic and magnetic regions are summarized in Table I. The parameter Δ in Table I describes the electric quadrupole interaction. For nonmagnetic spectra it stands for the quadrupole splitting, while for magnetic spectra it stands for $\frac{1}{4}(\frac{c}{E_0})eQ_eV_{zz}(3\cos^2\theta - 1)$. Here the symbol c stands for the speed of light in a vacuum, the

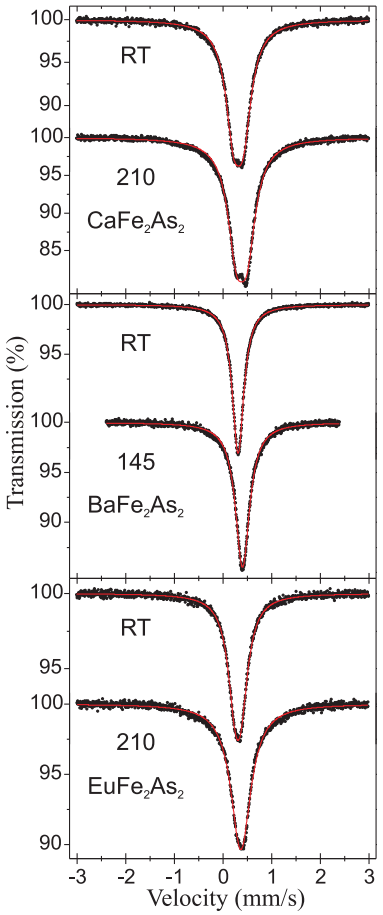

FIG. 1. (Color online) Mössbauer spectra in the "nonmagnetic" region.

symbol E_0 stands for the energy of the resonant transition, and the symbol e stands for a positive elementary charge. The symbol Q_e denotes the spectroscopic nuclear quadrupole moment in the excited nuclear state (positive for the first excited level in ^{57}Fe), while the symbol V_{zz} stands for the principal component of the electric field gradient (EFG) with the maximum absolute value. The angle $0 \leqslant \theta \leqslant \pi/2$ stands for the angle between the above EFG component and the hyperfine field under the assumption that the EFG is axially symmetric. Axial symmetry is expected for the tetragonal phase, while the orthorhombic distortion is too small to have a measurable effect on the EFG. The EFG component V_{zz} is expected to be positive here due to the local symmetry around the iron atom, and to be oriented perpendicular to the tetragonal (orthorhombic) plane. The above statement is consistent with the observed sign of the very slight asymmetry of doublets in the nonmagnetic region upon having taken into account the fact that absorber particles are composed of flat flakes likely to orient in the absorber plane. The tetragonal (orthorhombic) axis is perpendicular to the flake surface, of course. Hence, one can conclude that the hyperfine field is likely to be oriented closer to the orthorhombic plane than to the tetragonal (orthorhombic) axis as the angle θ exceeds the magic angle. The quadrupole interaction parameter is not quoted for the nonmagnetic spectrum of the $EuFe_2As_2$ compound obtained at 210 K, as it cannot be determined reliably due to the onset of magnetic order. One can use the full diagonalization of the hyperfine Hamiltonian, but such a procedure cannot be applied here as the electric quadrupole and magnetic dipole interactions are both very small and their parameters cannot be obtained reliably due to the limited resolution (i.e., due to finite line width). The quadrupole interaction in $BaFe_2As_2$ is too small to be observed without having a sufficiently strong magnetic field. The spectral shift S evolves with temperature mainly due to the second order Doppler shift (SOD). However, one can see a slight decrease of the shift at the transition from tetragonal to orthorhombic phase (i.e., an electron density on the iron nucleus slightly increases while transforming from the tetragonal to orthorhombic phase). A similar effect, albeit of the opposite sign, was observed in the FeSe superconductor.[2]

Figures 2 through 4 show spectra within the temperature range with magnetic order. Each spectrum is accompanied by a corresponding diagram showing SDW shape and by the resulting histogram of the field distribution $W(B)$. The average fields $\langle|B|\rangle$ derived from histograms are shown for each histogram. In fact, such an average field equals the average field calculated from the distribution of the absolute values of the hyperfine fields. Some common features could be recognized for all compounds investigated. For temperatures just below the transition temperature to the magnetically ordered state, the SDW is composed of thin sheets with a large volume of the crystal having a very small amplitude of the spin density. However, the maximum amplitude is not very much smaller than at saturation (about 70% of the saturation value). Upon lowering the temperature, magnetic sheets expand mainly at the base leading to the quasitriangular shape, and finally quasirectangular shape occurs. Quasitriangular behavior is definitely less pronounced for the barium compound, and hence less harmonics suffice to describe the spectrum. On the other hand, the calcium compound does not develop a fully quasirectangular shape even at liquid helium temperature. It is worth noting that SDW fully develops to the quasirectangular shape in a much narrower temperature range for the barium compound in comparison with the calcium and europium compounds. The quality of fits is somewhat diminished in the quasirectangular region of SDW, as the latter spectra tend to be indistinguishable from the spectra due to the unique field. However, one can be confident about the SDW model integrity due to the shape of the higher temperature spectra. Finally, one has to bear in mind that SDW amplitudes seen by resonant nuclei are rescaled by the (almost) constant factor due to the core polarization. Hence, amplitudes in the absence of the atomic core and resulting magnetic moments cannot be simply estimated without detailed calculations of the iron electronic states all the way down to the deepest shells. The evolution of the SDW shape is seen in the relative units qx, and hence evolution in the absolute units of distance is additionally dependent on the variation of the wave number (wavelength) with the temperature.

Figure 5 shows a comparison between the hyperfine field distribution derived from SDW and a similar (normalized to unity) distribution obtained by means of the Hesse-Rübartsch (HR) method in the Lorentzian approximation and with the quadrupole interaction included to the first order approximation.[23,24] The optimum smoothing filter and number

TABLE I. Essential parameters derived from the Mössbauer spectra. The symbol T denotes temperature. The symbol S denotes total shift (including second order Doppler shift) versus room temperature α-Fe, while the symbol Δ stands for the parameter describing electric quadrupole interaction (see text for details). Symbols h_{2n-1} stand for the amplitudes of SDW harmonics. Values of the harmonic amplitudes quoted in brackets $\langle \ldots \rangle$ are obtained setting amplitudes of ten subsequent odd harmonics equal to the amplitude of the last quoted harmonic. Above common amplitude was used as variable. Such procedure was essential to reproduce quasirectangular shapes of SDW with high accuracy. Absorber line widths were used as 0.16 mm/s for Ca, 0.15 mm/s for Ba, and 0.17 mm/s for Eu compounds in the magnetic region.

T(K) ±0.01	S(mm/s) ±0.001	Δ(mm/s) ±0.002	h_1(T) ±0.01	h_3(T) ±0.02	h_5(T) ±0.03	h_7(T) ±0.03	h_9(T) ±0.03	h_{11}(T) ±0.03	h_{13}(T) ±0.03
$CaFe_2As_2$									
RT	0.434	0.194							
210	0.499	0.212							
180	0.517	−0.044	5.39	−2.05	1.05	0.12	0.23		
170	0.516	−0.078	7.17	−1.64	0.10	0.21	0.24	−0.06	0.16
165	0.510	−0.094	8.01	−1.15	−0.24	0.06	0.31	−0.02	0.08
160	0.511	−0.096	8.63	−0.71	−0.34	−0.12	0.30	0.01	0.10
155	0.508	−0.098	9.10	−0.35	−0.32	−0.20	0.25	0.03	0.11
145	0.514	−0.094	9.74	0.13	−0.26	−0.32	0.18	0.01	0.17
120	0.531	−0.090	10.71	0.99	−0.17	−0.35	0.23	−0.29	0.28
80	0.550	−0.092	11.56	1.65	0.23	−0.30	0.07	−0.27	0.19
4.2	0.566	−0.092	12.41	2.45	0.80	−0.02	0.46	−0.30	0.03
$BaFe_2As_2$									
RT	0.426	0							
145	0.517	0							
141	0.518	−0.004	1.39	−1.18	0.83				
139	0.519	−0.014	1.70	−1.42	0.95				
137	0.517	−0.028	3.31	−0.92	−0.45				
135	0.515	−0.028	4.41	1.08	0.11	−0.46			
133	0.520	−0.030	4.75	1.89	0.45	0.79			
131	0.520	−0.030	5.01	1.92	0.62	0.71			
129	0.521	−0.030	5.24	2.03	0.68	0.74	0.17		
125	0.522	−0.030	5.31	2.19	0.79	1.06	0.36	0.64	
105	0.536	−0.032	5.95	2.66	0.88	1.26	0.44	0.72	⟨0.25⟩
80	0.540	−0.034	6.68	1.97	0.94	⟨0.42⟩			
4.2	0.552	−0.038	6.90	2.15	1.11	⟨0.44⟩			
$EuFe_2As_2$									
RT	0.425	0.118							
210	0.483								
200	0.487	−0.058	3.64	−2.78	0.27				
195	0.488	−0.070	4.96	−1.80	0.33	0.42	0.40		
193	0.490	−0.062	5.41	−1.56	0.02	0.27	0.41		
191	0.483	−0.088	6.14	−0.96	−0.30	−0.11	0.25		
189	0.477	−0.082	6.89	−0.29	−0.15	−0.29	0.15		
187	0.482	−0.088	7.27	0.17	−0.02	−0.32	0.06		
185	0.485	−0.086	7.52	0.49	0.10	−0.26	0.04		
180	0.494	−0.094	8.12	1.07	0.42	−0.10	0.16		
170	0.501	−0.096	8.65	2.14	0.53	−0.15	0.21	0.55	
145	0.520	−0.104	8.86	3.90	1.21	1.93	0.49	0.44	
80	0.540	−0.120	9.50	4.20	1.40	1.96	0.61	0.96	0.30
4.2	0.552	−0.116	10.67	3.23	1.61	0.89	0.43	0.43	⟨0.43⟩

of histogram points extended over the complete range of the hyperfine field have been applied in the case of HR analysis. The field range for HR data processing was set from zero to $B_{\max}$ of the corresponding distribution due to SDW. Hence the scale of the hyperfine field ranges from $-\frac{1}{2}\Delta B_{\mathrm{HR}}$ till $B_{\max} + \frac{1}{2}\Delta B_{\mathrm{HR}}$ in equal steps ΔB_{HR} in the case of the HR method. The HR method is generally recognized as the best numerical approach to the spectra exhibiting field distribution of the unknown origin. The lower plots of Fig. 5 show HR distributions for selected spectra, while the upper plots show $W(B)$, the latter resulting from SDW for the same spectra. One could see that the average field $\langle |B| \rangle$ is reproduced rather accurately by the HR method, but the shape of the distribution is poorly reproduced–particularly in the flat regions. The gross maxima of the distributions due to the SDW are reproduced approximately by the HR method. Fits are of a comparable quality, but the HR method does not give a physical insight into the problem and one cannot go back from the hyperfine field distribution to the shape of the SDW, as the reciprocal transformation is not unique.

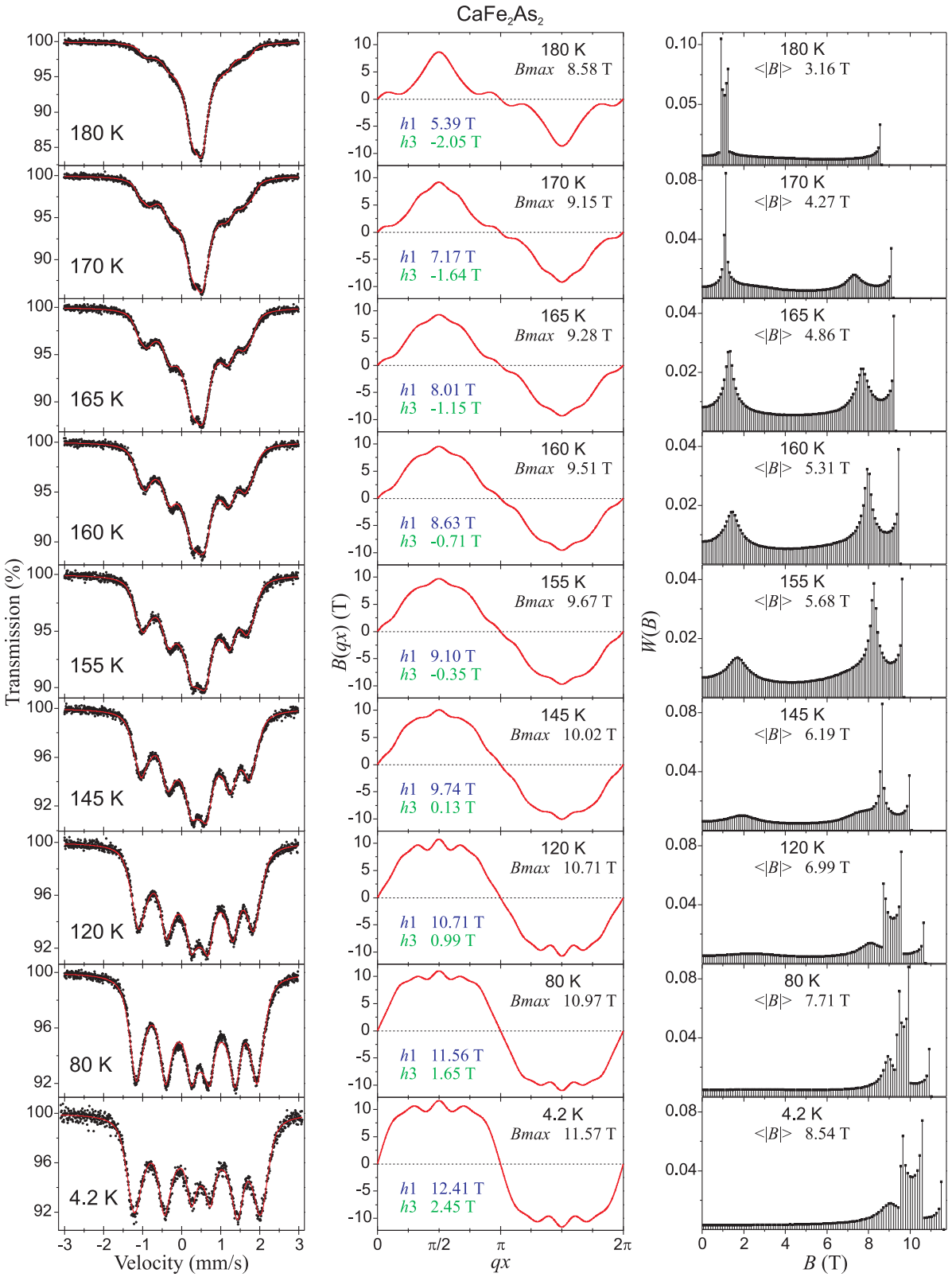

FIG. 2. (Color online) Mössbauer spectra, SDW shapes, and resulting hyperfine field distributions for $CaFe_2As_2$ in the magnetically ordered region versus temperature. Amplitudes of the first two harmonics h_1 and h_3 are listed on corresponding plots of SDW shape. Symbol $\langle|B|\rangle$ stands for the average of the respective field distribution, while $B_{\max}$ denotes maximum value of SDW.

Figure 6 shows $\sqrt{\langle B^2\rangle}$ versus temperature for all compounds investigated. This parameter is, in principle, proportional to the square root from the intensity of the magnetic Bragg reflection in the neutron scattering—provided that other

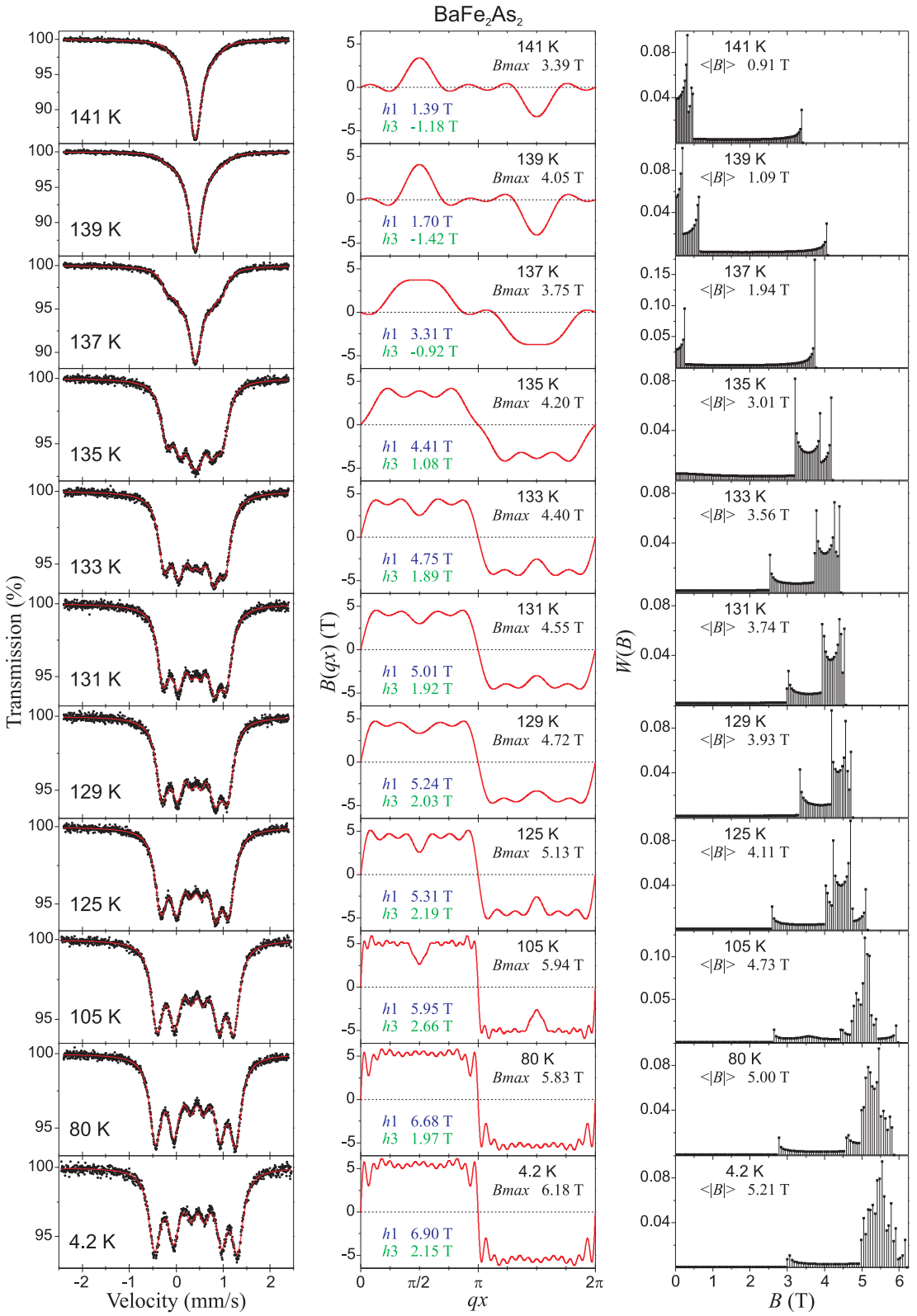

FIG. 3. (Color online) Mössbauer spectra, SDW shapes, and resulting hyperfine field distributions for $BaFe_2As_2$ in the magnetically ordered region versus temperature.

electronic magnetic moments than due to SDW are absent and q remains fairly constant.[11] Hence, the parameter $\sqrt{\langle B^2 \rangle}$ is proportional to the value of the electronic magnetic moment per unit volume. It is evident that magnetic ordering of europium at low temperature (at about 19 K) has no effect on the magnetism of 3*d* electrons.

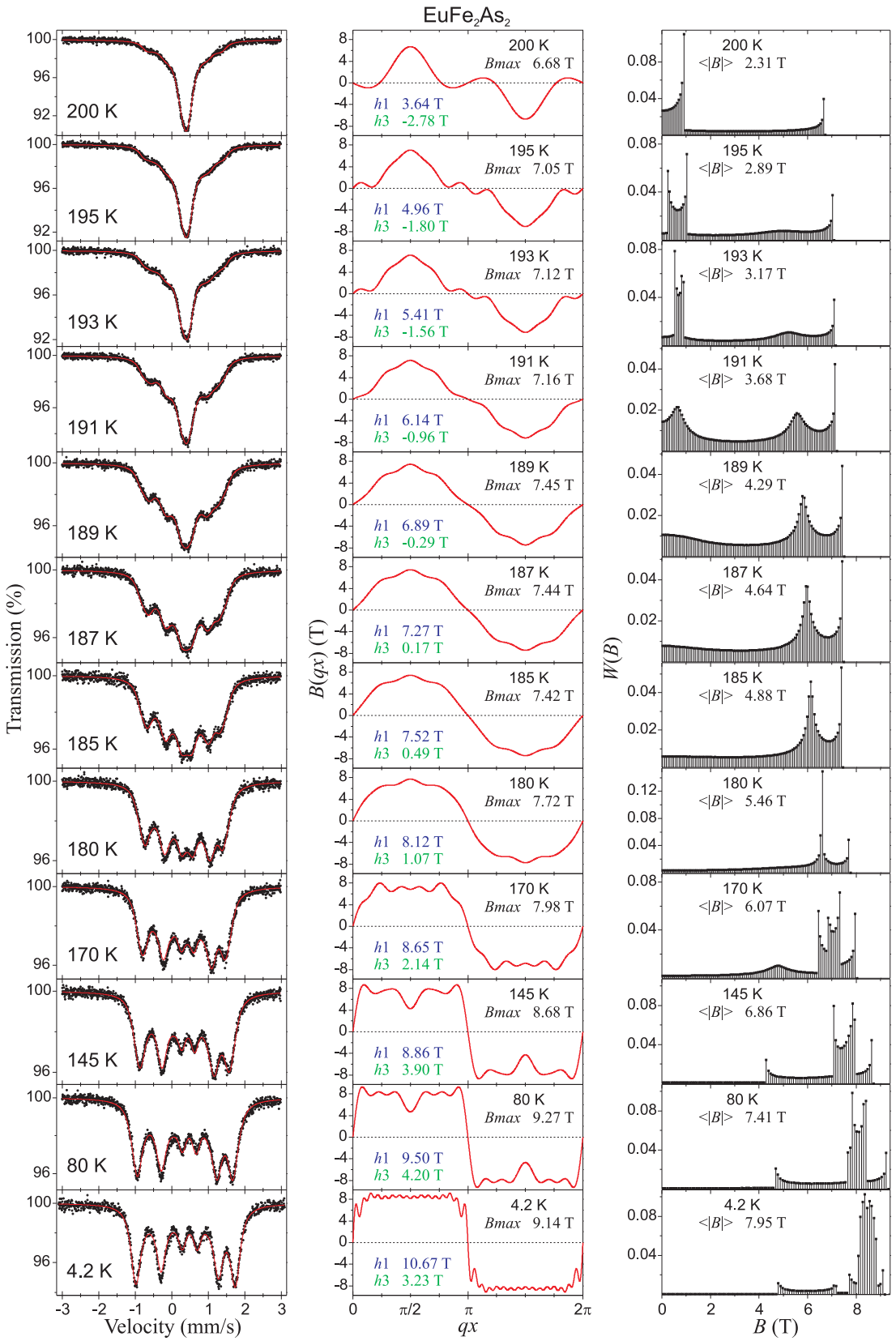

FIG. 4. (Color online) Mössbauer spectra, SDW shapes, and resulting hyperfine field distributions for $EuFe_2As_2$ in the magnetically ordered region versus temperature.

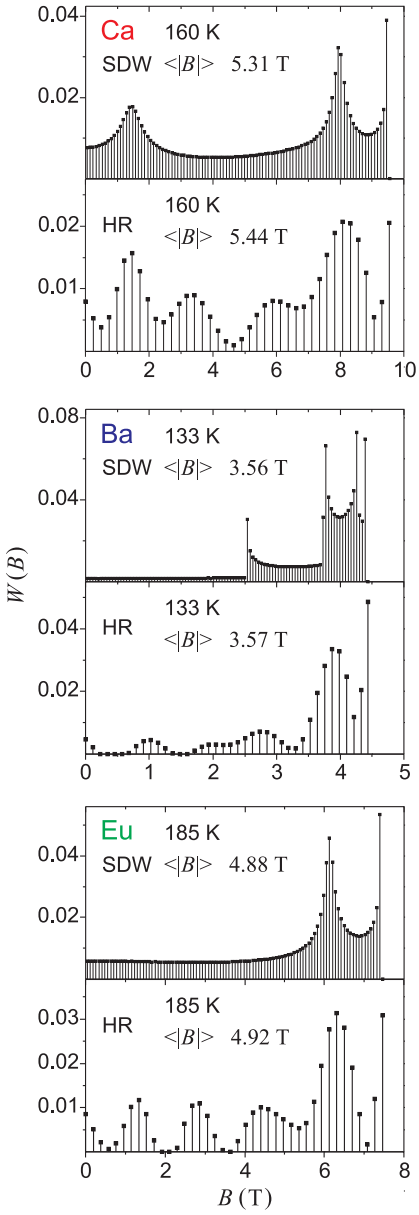

FIG. 5. (Color online) Comparison of the hyperfine field distribution resulting from SDW shape with the corresponding field distribution yielded by the HR method for selected spectra.

It seems that the parameter $\sqrt{\langle B^2\rangle}$ behaves versus temperature T like the power function of the following type:

$$\sqrt{\langle B^2\rangle} = B_0\left(1-\frac{T}{T_c}\right)^{\alpha} \quad \text{for} \quad 0 \leqslant \frac{T}{T_c} \leqslant x_0 \quad \text{and}$$
$$\sqrt{\langle B^2\rangle} = B_0 A\left(\frac{T}{T_c}\right)^{-\beta} \quad \text{for} \quad \frac{T}{T_c} \geqslant x_0 \qquad (5)$$
$$\text{with} \quad x_0 = \frac{\beta}{\alpha_0+\beta} \quad \text{and} \quad A = x_0^{\beta}(1-x_0)^{\alpha_0}.$$

The symbol $B_0 > 0$ denotes the saturation value of the ground state, while the symbol $T_c > 0$ denotes the transition temperature to the high temperature state. The low temperature (critical) exponent satisfies the following condition $0 < \alpha < 1$. The high temperature exponent β is also positive and

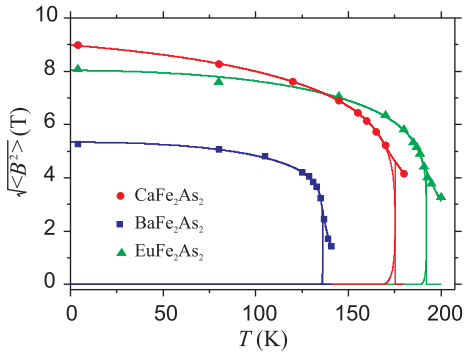

FIG. 6. (Color online) Plot of square root from the mean squared amplitude of SDW $\sqrt{\langle B^2\rangle}$ versus temperature. Solid lines represent total, coherent, and incoherent contributions as described in the text. Error bars for both field and temperature are smaller than the symbol size.

usually one can expect $\beta > 1$. It is hard to expect that the low temperature exponent remains constant within the whole applicable temperature range. Improved fits can be obtained setting $\alpha = \alpha_0[(1-\gamma)+\gamma(T/T_0)]$ for $0 \leqslant T < T_0$ and $\alpha = \alpha_0$ for $T \geqslant T_0$, where the following conditions are satisfied: $0 < \alpha_0 < 1$ and $0 \leqslant \gamma < 1$. The temperature T_0 is defined as $T_0 = x_0 T_c$, while the parameter α_0 approximates the low temperature critical exponent. It is assumed here that the following condition is satisfied $(T_c - T_0)/T_c \ll 1$. It is unlikely that the high temperature tail extending till the transition (with some hysteresis) from the low temperature orthorhombic phase to the magnetically disordered high temperature tetragonal phase is due to the critical fluctuations as it is too large (i.e., it represents relatively too strong field). On the other hand, critical fluctuations lead to the more or less homogeneous broadening of the Mössbauer spectrum, which are inconsistent with the observed spectrum shape within this temperature region. It rather seems that this tail is due to the SDW having a short coherence length, and hence is invisible by the diffraction-based methods like coherent neutron scattering. On the other hand, local methods like the Mössbauer spectroscopy are completely insensitive to the time-independent incoherence of SDW. Therefore $\beta > 1$ is expected, in contrast to the case of critical fluctuations. Hence, for coherent neutron scattering one is likely to see some quantity proportional to the following function:

$$\sqrt{\langle B^2\rangle_C} = B_0\left(1-\frac{T}{T_c}\right)^{\alpha} \quad \text{for} \quad 0 \leqslant \frac{T}{T_c} \leqslant 1 \quad \text{and}$$
$$\sqrt{\langle B^2\rangle_C} = 0 \quad \text{for} \quad \frac{T}{T_c} \geqslant 1. \qquad (6)$$

Equation (5) yields the same result as Eq. (6) for $T/T_c \leqslant x_0$. The functions described by the above equations bifurcate at temperature $T_0 < T_c$, that is, below temperature T_0 the incoherent contribution vanishes, while above temperature T_c the coherent contribution vanishes. The field at temperature T_0 takes on the value $B_F = B_0(\frac{\alpha_0}{\alpha_0+\beta})^{\alpha_0}$. The coherent and incoherent contributions equal each other at temperature $T_t = x_t T_c$, where $T_0 < T_t < T_c$. The parameter x_t is the solution of the equation $Ax_t^{-\beta} - 2(1-x_t)^{\alpha_0} = 0$ from the range

$x_0 < x_t < 1$. The total field B_t at temperature T_t is composed of coherent and incoherent contributions in equal amounts. The above discrepancy between coherent and local methods has been already mentioned by Bonville *et al.*[11]. It is interesting to note as well that Eq. (5) yields the following asymptotic form close to the ground state:

$$\lim(\sqrt{\langle B^2\rangle})_{T/T_c\to+0} = B_0\Bigg[1-\alpha_0(1-\gamma)\left(\frac{T}{T_c}\right)-\frac{1}{2} \times\left(\alpha_0(1-\gamma)[1-\alpha_0(1-\gamma)] +\frac{2\alpha_0\gamma T_c}{T_0}\right)\left(\frac{T}{T_c}\right)^2+\cdots\Bigg]. \quad (7)$$

The linear behavior of Eq. (7) versus temperature close to the ground state can be seen unless $\alpha_0(1-\gamma)\approx 0$. The essential results of fits are summarized in Table II. The linear dependence close to the ground state is clearly seen for $CaFe_2As_2$, while for the remaining compounds the condition $\alpha_0(1-\gamma)\approx 0$ is approximately satisfied as SDW close to the ground state has an almost rectangular shape. For these compounds quasiantiferromagnetic conditions are reached in contrast to $CaFe_2As_2$. Hence, the itinerant character of magnetic order is pronounced, at most, for $CaFe_2As_2$. It is interesting to note that the critical exponent α_0 is quite close to the critical exponent ($\sim$0.125) of the antiferromagnetic system having one dimension in the spin space and two dimensions in the real space. The unidimensional spin space is consistent with the SDW being a planar wave with definite spin polarization (i.e., for the unique direction of the spin orientation). Two dimensions in the real space mean that the exchange interaction leading to the magnetic order is predominantly confined to (orthorhombic) planes and it seems that the coupling between planes weakens while going from A = Ca through Eu to Ba. The same universality class (1,2) with unidimensional electronic spin space and two-dimensional real space has been found for $EuFe_2As_2$ by Raffius *et al.*,[25] as far as the 3*d* magnetic order is concerned. Note that the exponent β increases drastically, while going from Ca through Eu to Ba. It means that magnetic order is more and more confined to the orthorhombic plane when calcium is replaced by europium and subsequently by barium. Such behavior correlates with the lattice period along the orthorhombic axis. This lattice constant is $c = 11.725$ Å for $CaFe_2As_2$ (Ref. 18), $c = 12.085$ Å for $EuFe_2As_2$ (Ref. 19), and $c = 13.017$ Å for $BaFe_2As_2$ (Ref. 6) in the tetragonal phase at room temperature. The presence of the magnetic tail can be due to the coexistence of the magnetically disordered tetragonal phase and magnetically ordered orthorhombic phase exhibiting a small magnetic hyperfine field. However, this interpretation does not seem likely for the following reasons. First of all, no irreversibility of the parameter $\sqrt{\langle B^2\rangle}$ versus temperature was found near the transition temperature. Furthermore, coherent regions of the parent/daughter phase are likely to have a size comparable with the size of the crystallite or domain in the case of a large single crystal. This size exceeds the typical coherence length of the neutron scattering method, while the tail is still invisible by the neutron scattering method.[26] The nuclear magnetic resonance (NMR) results obtained by means of the ^{75}As nuclear probe are less conclusive due to the complex mechanism leading to the transferred hyperfine field on the As nucleus.[27–29]

It seems that a similar kind of magnetic order occurs in other parents or underdoped compounds leading to the iron-based superconductivity provided they behave like metals. In particular, Mössbauer iron spectra of the 1111 family are quite similar for the magnetically ordered phases.[1,9,10,17] Some of them were interpreted as due to several (or single) precisely defined fields, but such a treatment does not seem justified while looking for the evolution of the spectrum shape with temperature. Another explanation was given interpreting spectra within the framework of the spin fluctuations (i.e., as the relaxation spectra).[10] Such fluctuations are unlikely to be observable on the so long time scale as the time scale of the hyperfine interactions. The overall density of electronic spins is high, magnetic order develops at rather high temperatures, and the system is metallic. Hence, the relaxation has to occur on much shorter time scales leading to the semiclassical average field in the conduction band. Relaxation is mainly due to the spin-spin interactions with a very small lattice contribution as the system has itinerant electrons. Hence, there is no way to explain the dependence of the relaxation time on temperature. Even rare earths (if present as constituents) develop rather hyperfine fields due to long-range order instead of coupling between the nucleus and the local 4*f* shell despite the fact that 4*f* electrons are weakly coupled to the conduction band.[10,30,31] It seems that sample inhomogeneity leading subsequently to magnetic clusters and hyperfine field distribution can be ruled out at least for parent compounds, as the latter are highly ordered structures from the crystallographic point of view. Other mechanisms of magnetic ordering like spin glass formation are even less probable for the compounds in question due to the strongly layered structure.

TABLE II. Essential parameters describing evolution of $\sqrt{\langle B^2\rangle}$ versus temperature. Note, that parameter B_0A stands for the incoherent field at temperature T_c. Fitted parameters are B_0, T_c, α_0, γ, and β. Remaining parameters are derived based on the values of the fitted parameters. Errors for parameters B_t and T_t have not been estimated as these parameters depend on the numerical solution of the nonlinear equation—see text for details. Transition temperatures T_c are close to those reported in the literature, i.e., 171 K for $CaFe_2As_2$ (Ref. 4), 140 K for $BaFe_2As_2$ (Ref. 6), and 190 K for $EuFe_2As_2$ (Ref. 5).

Compound	$CaFe_2As_2$	$BaFe_2As_2$	$EuFe_2As_2$
B_0(T)	8.98(2)	5.34(1)	8.03(2)
B_F(T)	5.4(1)	3.1(1)	4.8(1)
B_t(T)	4.62	2.81	4.25
B_0A(T)	4.62(3)	2.81(2)	4.25(2)
T_c(K)	175.3(3)	136.0(1)	192.1(1)
T_t(K)	175.2	136.0	192.1
T_0(K)	168.3(4)	135.3(1)	189.1(1)
α_0	0.158(2)	0.102(1)	0.124(1)
γ	0.3(1)	1.0(1)	0.9(1)
β	3.8(1)	20.4(4)	7.6(1)

V. CONCLUSION

The study of the evolution of the Mössbauer spectra versus temperature for AFe_2As_2 (A = Ca, Ba, Eu) parent compounds of the 122 family of iron-based superconductors leads to the conclusion that 3*d* magnetism of these compounds is due to the development of SDW below the transition temperature. The shape of SDW evolves significantly with temperature forming narrow sheets of significant spin density at the onset of the transition. The magnetic sheets broaden subsequently passing in some cases through the semitriangular shape of SDW. Finally, a quasirectangular shape is formed and spectra are almost the same as for the single precisely defined field, the latter being characteristic of the classical antiferromagnet (and ferromagnet as well). It seems that such behavior is a common feature for all parents and related underdoped compounds (e.g., also for the 1111 family). No measurable charge density waves (CDW) were found, at least in the bulk of the material, which contribute most of the signal in the transmission Mössbauer spectroscopy.

The critical exponent α_0 cannot be determined very accurately due to the presence of the tail above magnetic transition and, in fact, it is rather underestimated. However, its value indicates without any doubt that these compounds belong to the universality class (1,2) as far as the magnetic order is considered. The tail is likely to be due to the presence of incoherent SDW in a relatively narrow temperature range around the transition point.

There is no measurable contribution to the magnetic hyperfine field on iron due to the magnetic ordering of the europium ions. Recently a small transferred field on iron due to the europium ordering was found in $EuFe_2(As_{1-x}P_x)_2$ even in the superconducting state with diamagnetic iron accompanied by the generation of the significant electric quadrupole interaction on iron owing to the replacement of As by P (Ref. 32).

The formation of the magnetically ordered sheets separated by almost nonmagnetic layers is a prerequisite to the formation of the Fulde-Ferrell-Larkin-Ovchinnikov (FFLO) phase.[33,34] However, nonmagnetic regions do not exhibit superconductivity for the compounds in question, and upon lowering temperature the system orders in the itinerant antiferromagnetic fashion, which is not necessarily commensurate. It seems that the SDW period in the real space is too small to allow the formation of the FFLO phase (i.e., the wave number q is too high for the systems investigated).

ACKNOWLEDGMENTS

Jakub Cieślak from the Faculty of Physics and Applied Computer Science, AGH University of Science and Technology, Kraków, Poland is thanked for informative discussions.

*Corresponding author: sfrueben@cyf-kr.edu.pl

[1] S. Kitao, Y. Kobayashi, S. Higashitaniguchi, M. Saito, Y. Kamihara, M. Hirano, T. Mitsui, H. Hosono, and M. Seto, J. Phys. Soc. Jpn. **77**, 103706 (2008).

[2] A. Błachowski, K. Ruebenbauer, J. Żukrowski, J. Przewoźnik, K. Wojciechowski, and Z. M. Stadnik, J. Alloys Compd. **494**, 1 (2010).

[3] M. Rotter, M. Tegel, I. Schellenberg, F. M. Schappacher, R. Pöttgen, J. Deisenhofer, A. Günther, F. Schrette, A. Loidl, and D. Johrendt, New J. Phys. **11**, 025014 (2009).

[4] F. Ronning, T. Klimczuk, E. D. Bauer, H. Volz, and J. D. Thompson, J. Phys. Condens. Matter **20**, 322201 (2008).

[5] M. Tegel, M. Rotter, V. Weiß, F. M. Schappacher, R. Pöttgen, and D. Johrendt, J. Phys. Condens. Matter **20**, 452201 (2008).

[6] M. Rotter, M. Tegel, D. Johrendt, I. Schellenberg, W. Hermes, and R. Pöttgen, Phys. Rev. B **78**, 020503(R) (2008).

[7] Y. Laplace, J. Bobroff, F. Rullier-Albenque, D. Colson, and A. Forget, Phys. Rev. B **80**, 140501(R) (2009).

[8] F. L. Ning, K. Ahilan, T. Imai, A. S. Sefat, R. Jin, M. A. McGuire, B. C. Sales, and D. Mandrus, Phys. Rev. B **79**, 140506(R) (2009).

[9] H.-H. Klauss, H. Luetkens, R. Klingeler, C. Hess, F. J. Litterst, M. Kraken, M. M. Korshunov, I. Eremin, S.-L. Drechsler, R. Khasanov, A. Amato, J. Hamann-Borrero, N. Leps, A. Kondrat, G. Behr, J. Werner, and B. Büchner, Phys. Rev. Lett. **101**, 077005 (2008).

[10] P. Wang, Z. M. Stadnik, C. Wang, G.-H. Cao, and Z.-A. Xu, J. Phys. Condens. Matter **22**, 145701 (2010).

[11] P. Bonville, F. Rullier-Albenque, D. Colson, and A. Forget, EPL **89**, 67008 (2010).

[12] I. Nowik, I. Felner, Z. Ren, Z.-A. Xu, and G.-H. Cao, J. Phys.: Conf. Series **217**, 012121 (2010).

[13] S. Sharma, A. Bharathi, S. Chandra, V. R. Reddy, S. Paulraj, A. T. Satya, V. S. Sastry, A. Gupta, and C. S. Sundar, Phys. Rev. B **81**, 174512 (2010).

[14] N. Kumar, R. Nagalakshmi, R. Kulkarni, P. L. Paulose, A. K. Nigam, S. K. Dhar, and A. Thamizhavel, Phys. Rev. B **79**, 012504 (2009).

[15] Z. Li, X. Ma, H. Pang, and F. Li, e-print arXiv:1004.4328v1 (2010).

[16] M. Tegel, S. Johansson, V. Weiß, I. Schellenberg, W. Hermes, R. Pöttgen, and D. Johrendt, EPL **84**, 67007 (2008).

[17] D. R. Sánchez, M. Alzamora, J. Munevar, N. L. Wang, G. F. Cheng, and E. Baggio-Saitovitch, J. Phys. Condens. Matter **21**, 455701 (2009).

[18] M. Matusiak, Z. Bukowski, and J. Karpinski, Phys. Rev. B **81**, 020510(R) (2010).

[19] Z. Guguchia, J. Roos, A. Shengelaya, S. Katrych, Z. Bukowski, S. Weyeneth, F. Murányi, S. Strässle, A. Misuradze, J. Karpinski, and H. Keller, e-print arXiv:1010.5948v1 (2010).

[20] J. G. Storey, J. W. Loram, J. R. Cooper, Z. Bukowski, and J. Karpinski, e-print arXiv:1001.0474v1 (2010).

[21] J. Cieślak and S. M. Dubiel, Nucl. Instrum. Methods B **95**, 131 (1995); J. Cieślak, Ph.D. Thesis, AGH University of Science and Technology, Kraków, Poland, 1995.

[22] K. Ruebenbauer and Ł. Duraj [www.elektron.up.krakow.pl/mosgraf-2009].

[23] J. Hesse and A. Rübartsch, J. Phys. E: Sci. Instrum. **7**, 526 (1974).

[24]G. Le Caër and J. M. Dubois, J. Phys. E: Sci. Instrum. **12**, 1083 (1979).
[25]H. Raffius, E. Mörsen, B. D. Mosel, W. Müller-Warmuth, W. Jeitschko, L. Terbüchte, and T. Vomhof, J. Phys. Chem. Solids **54**, 135 (1993).
[26]M. Kofu, Y. Qiu, W. Bao, S.-H. Lee, S. Chang, T. Wu, G. Wu, and X. H. Chen, New J. Phys. **11**, 055001 (2009).
[27]N. J. Curro, A. P. Dioguardi, N. Ap. Roberts-Warren, A. C. Shockley, and P. Klavins, New J. Phys. **11**, 075004 (2009).
[28]K. Kitagawa, N. Katayama, K. Ohgushi, M. Yoshida, and M. Takigawa, J. Phys. Soc. Jpn. **77**, 114709 (2008).
[29]H. Fukazawa, K. Hirayama, K. Kondo, T. Yamazaki, Y. Kohori, N. Takeshita, K. Miyazawa, H. Kito, H. Eisaki, and A. Iyo, J. Phys. Soc. Jpn. **77**, 093706 (2008).
[30]Anupam, P. L. Paulose, H. S. Jeevan, C. Geibel, and Z. Hossain, J. Phys. Condens. Matter **21**, 265701 (2009).
[31]D. H. Ryan, J. M. Cadogan, C. Ritter, F. Canepa, A. Palenzona, and M. Putti, Phys. Rev. B **80**, 220503(R) (2009).
[32]I. Nowik, I. Felner, Z. Ren, G. H. Cao, and Z. A. Xu, J. Phys. Condens. Matter **23**, 065701 (2011).
[33]P. Fulde and R. A. Ferrell, Phys. Rev. **135**, A550 (1964).
[34]A. I. Larkin and Yu. N. Ovchinnikov, Zh. Eksp. Teor. Fiz. **47**, 1136 (1964) [Sov. Phys. JETP **20**, 762 (1965)].